EXOSKELETONS

Modulation of Achilles tendon force with load carriage and exosuit assistance

Dylan G. Schmitz[1]†, Richard W. Nuckols[2]†‡, Sangjun Lee[2], Tunc Akbas[2], Krithika Swaminathan[2], Conor J. Walsh[2]§, Darryl G. Thelen[1]*§

Exosuits have the potential to assist locomotion in both healthy and pathological populations, but the effect of exosuit assistance on the underlying muscle-tendon tissue loading is not yet understood. In this study, we used shear wave tensiometers to characterize the modulation of Achilles tendon force with load carriage and exosuit assistance at the ankle. When walking (1.25 m/s) unassisted on a treadmill with load carriage weights of 15 and 30% of body weight, peak Achilles tendon force increased by 11 and 23%, respectively. Ankle exosuit assistance significantly reduced peak Achilles tendon force relative to unassisted, although the magnitude of change was variable across participants. Peak Achilles tendon force was significantly correlated with peak ankle torque for unassisted walking across load carriage conditions. However, when ankle plantarflexor assistance was applied, the relationship between peak tendon force and peak biological ankle torque was no longer significant. An outdoor pilot study was conducted in which a wearable shear wave tensiometer was used to measure Achilles tendon wave speed and compare across an array of assistance loading profiles. Reductions in tendon loading varied depending on the profile, highlighting the importance of in vivo measurements of muscle and tendon forces when studying and optimizing exoskeletons and exosuits.

INTRODUCTION

Wearable robotic systems interact with users by applying force in parallel with muscle-tendon systems. When properly designed and implemented, this parallel assistance can be used in a variety of applications to aid the user. For example, both active (*1*–*3*) and passive (*4*, *5*) ankle assistance can offload the net biological ankle torque and reduce the energetic demand. In one study, an exosuit applying plantarflexion assistance reduced the metabolic cost of walking in healthy participants by 8 to 16% in a range of walking speeds and inclines compared with walking with no device (*3*). However, biomechanical and metabolic responses to robotic assistance remain highly variable, with individual responses sensitive to the timing and magnitude of assistance applied (*6*, *7*). Variability in responses becomes even more challenging when robotic devices are used for assistance in clinical populations, such as after stroke (*7*–*10*) or spinal cord injury (*11*, *12*).

The effectiveness of personalized wearable robotic systems is highly connected to how torque and forces are delivered to the user and the resulting effect on the neuromusculoskeletal system. Studies into exosuit biomechanics have traditionally used laboratory-based motion capture systems and instrumented force plates to estimate how musculoskeletal load is affected by parallel assistance. With this approach, a biological joint torque is calculated by subtracting the external exosuit or exoskeleton torque from the net joint torque computed via inverse dynamics. In walking with ankle exosuit assistance, biological ankle torque is reduced by the torque applied externally, which, for current exosuits, is up to 50% of the net ankle torque relative to unassisted walking (*1*). Numerous recent studies have shown that plantarflexion assistance is able to reduce biological ankle torque (*13*, *14*). However, biological ankle torque does not necessarily correspond directly to reductions in internal tissue forces. Exosuits can induce variations in kinematics, muscle coordination, and muscle-tendon dynamics (*13*, *14*), which, in turn, could affect the relationship between internal muscle-tendon force and biological ankle torque. Although inverse dynamics may indicate a substantial reduction in biological ankle torque, triceps surae force may not be reduced with applied assistance when, for example, the antagonist tibialis anterior (TA) cocontracts to stiffen the joint (*5*, *15*, *16*). Such complexities highlight the difficulty in reliably measuring and understanding the effect of exosuit assistance on tissue forces using indirect measures.

Exosuits are becoming increasingly portable and deployed in more dynamic and unconstrained environments. In contrast, traditional kinetic biomechanical assessments of exosuits are almost universally constrained to the laboratory, which limits the locomotor activities and saliency that can be considered. The exciting advances in robotics would benefit from parallel advances in wearable sensors that are usable outside the laboratory and provide quantitative in vivo muscle force measures by which robotic assistance could be assessed and tuned for individual users.

Shear wave tensiometry is a noninvasive method that can directly assess tendon force using a skin-mounted sensor. Past studies have shown that the speed, squared, of a shear wave traveling along a tendon modulates with the axial force in the tendon (*17*). This technique has been applied to dynamic human movement, and changes in Achilles tendon force have been quantified during walking and running in various conditions (*17*–*22*). Thus, because tensiometry is a direct measure of tendon force and independent of moment arms or muscle dynamics assumptions, it is feasible that shear wave tensiometry can be used to characterize the modulation of tissue forces with exosuit assistance. Furthermore, the sensor can

[1]Department of Mechanical Engineering, University of Wisconsin-Madison, Madison, WI, USA. [2]John A. Paulson School of Engineering and Applied Sciences, Harvard University, Cambridge, MA, USA.
*Corresponding author. Email: dgthelen@wisc.edu
†These authors contributed equally to this work.
‡Present address: Department of Systems Design Engineering, University of Waterloo, Waterloo, ON N2V 2K7, Canada.
§These authors contributed equally to this work.

be fabricated as a self-powered wearable device that can track tendon forces over long periods of time during outdoor locomotion.

In this study, we directly measured the Achilles tendon force in vivo during exosuit-assisted loaded walking. This direct measurement has numerous applications (*22*, *23*), including detection and mitigation of injury risk. Ground reaction forces increase proportionally with added load carriage weight (*24*), implying a corresponding increase in Achilles tendon force and a potential contributor to a heightened risk of injury (*24*). We measured the effect of load carriage on Achilles tendon force and the ability of the exosuit to then offset that additional force. We compared these results with the traditional measure of biological ankle joint torque. Inferring from previous literature (*25*), we hypothesized that Achilles tendon force would increase with load carriage and no assistance. We also hypothesized that exosuit assistance during load carriage would normalize Achilles tendon force toward baseline (unloaded) force. In an additional pilot study, we demonstrated how this tool can be used in combination with a portable ankle exosuit to understand how the exosuit assistance profile affects the Achilles tendon force in an unconstrained outdoor environment.

RESULTS

We conducted tests with eight healthy young adult participants [five females, age: 29.3 (3.8) mean (SD) years, mass: 70 (15.3) kg, height: 173.5 (12.2) cm]. Participants walked on a treadmill at 1.25 m/s for six conditions (Fig. 1). Participants walked with no assistance (SLK) and with exosuit assistance (EXO: 45% body weight peak force) (Fig. 2A) for each of the three load carriage conditions: 0% (no load), 15%, and 30% body weight (designated L00, L15, and L30, respectively). One participant exceeded the maximum force capacity of the exosuit at 45% body weight and instead performed the tests with a peak exosuit force of 30% body weight. We measured Achilles tendon shear wave speed, joint kinematics and kinetics, and electromyography (EMG). Shear wave speed was measured with shear wave tensiometry and calibrated to Achilles tendon force based on the SLK exosuit condition for each load carriage (fig. S1). We then used the participant-specific tensiometer calibrations to characterize Achilles tendon force from wave speed during exosuit-assisted walking trials. This calibration accounts for participant-specific physiological properties while preserving comparisons between conditions.

Load carriage with no exosuit assistance

As expected, both Achilles tendon shear wave speed and biological ankle torque increased significantly with load carriage during walking (Fig. 2B). Before calibration, median peak Achilles tendon shear wave speed squared increased by 14.0 and 23.4% for the L15 and L30 conditions, respectively, relative to L00. After calibration, peak Achilles tendon force, predicted by shear wave speed, increased by 11.0% ($P = 0.0012$) and 23.1% ($P < 0.0001$) for L15 and L30 relative to L00, respectively. Similarly, peak ankle torque increased by 12.8% ($P < 0.0001$) and 25.1% ($P < 0.0001$) for L15 and L30 load carriage conditions relative to L00, respectively.

Muscle activation in the soleus (SOL), medial gastrocnemius (MG), lateral gastrocnemius (LG), and TA did not show a significant increase with load carriage. Consequently, there was no correlation between muscle activation and Achilles tendon force with load carriage. The lack of relationship between ankle muscle activity and magnitude of load carriage may reflect the complexity of the dynamic EMG-force relationship (*26*) and variability in individual adaptation to alterations in load and joint dynamics (*27*–*29*).

Load carriage with exosuit assistance

In comparison with an increase in peak net ankle torque of 0.23 and 0.45 N·m/kg (12.8 and 25.1% relative to L00, respectively) for the unassisted L15 and L30 load carriage conditions (Fig. 3A), the exosuit applied an average peak torque of 0.29 N·m/kg. Peak Achilles tendon force with EXO was significantly reduced across load carriage conditions and participants ($P < 0.0001$) (Fig. 3B). However, there was substantial interparticipant variability in peak Achilles tendon force in response to exosuit assistance, with some participants exhibiting up to a 33% reduction in peak Achilles tendon force, whereas other participants showed increases in Achilles tendon force (Fig. 3C). On average, there were Achilles tendon force reductions of 4.8 and 3.4% for the L15 and L30 load carriage conditions, respectively (Fig. 3B). Biological ankle torque (measured by subtracting exosuit torque from total ankle joint moment measured by inverse dynamics) showed larger relative reductions with exosuit assistance compared with those observed in Achilles tendon force. Relative to SLK, peak biological ankle torque was reduced by 9% ($P = 0.0021$), 10% ($P = 0.0008$), and 11% ($P = 0.0086$) for the L00, L15, and L30 conditions, respectively (Fig. 3C and table S1). However, there was also interparticipant variability in peak biological ankle torque, with reductions ranging from 3 to 17% with exosuit assistance.

The effect of exosuit assistance on Achilles tendon force was strongest in the load carriage conditions, which caused a significant interaction effect between exosuit assistance and load carriage ($P = 0.0035$). Nominally, the L00 condition showed the least amount of change in Achilles tendon force with exosuit assistance, so the model was rerun to include only the L15 and L30 conditions. With this change, the interaction effect was not significant ($P = 0.46$). As with the load carriage conditions, exosuit assistance did not have a significant effect on muscle activation for the SOL, MG, LG, or TA. Furthermore, there were no significant relationships between changes in biological ankle torque due to exosuit assistance and muscle activation. Similarly, there were no significant relationships between changes in Achilles tendon force and muscle activation. The variable effects of assistance across participants, as well as the aforementioned complexities of muscle activation and force production, may be responsible for the absence of these relationships.

Ankle and knee kinematics

Ankle and knee kinematics were largely unaffected by load carriage (fig. S2). Ankle angle exhibited a minor shift toward greater dorsiflexion during early stance, but otherwise, ankle and knee kinematics were largely unaffected by load carriage. Knee angle was also unchanged by exosuit assistance. Ankle angle showed a reduction in dorsiflexion when assistance was applied.

Relationship between Achilles tendon force and ankle torque

Changes in peak Achilles tendon force were significantly correlated with changes in peak ankle torque when walking with load carriage without exosuit assistance (Fig. 4A). However, when exosuit

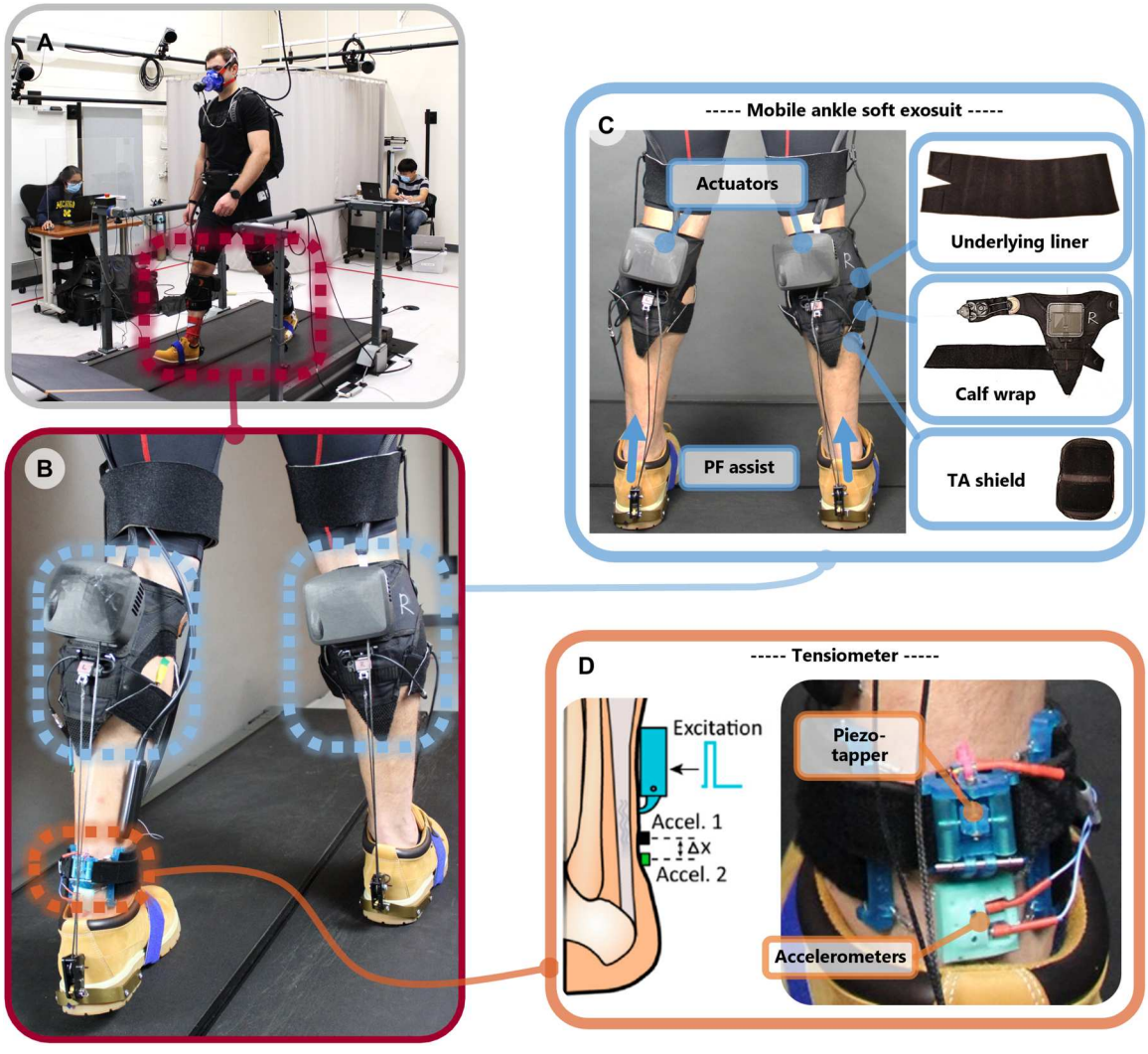

Fig. 1. Exosuit and tensiometer equipment. (**A**) Photo of the laboratory during the study. (**B**) The exosuit and tensiometer worn by a participant, with adhesive wrapping removed to show detail. (**C**) The mobile ankle soft exosuit consisted of a calf wrap secured over an underlying liner and shield to protect the TA from constrictive forces when the exosuit was active. The exosuit pulley system attached to the heel of a low-cut boot. PF, plantarflexion. (**D**) The shear wave tensiometer was placed on the left Achilles tendon above the boot.

assistance was applied, the relationship between Achilles tendon force and biological ankle torque was diminished. Peak Achilles tendon force tended to increase with peak biological ankle torque, but to a lesser degree, and the effects were not significant across load carriage conditions (Fig. 4B).

Modulating Achilles tendon force by varying exosuit assistance in overground walking

A pilot outdoor collection with a single participant was performed to assess the potential to tune exosuit control based on Achilles tendon force measurements in an unconstrained outdoor environment (Fig. 5). The participant walked outdoors on a level, paved course at about 1.25 m/s, following a researcher who set the pace. Nine exosuit plantarflexion assistance profiles were supplied by a mobile exosuit, defined by the time of torque onset, T1 [35, 40, and 45% gait cycle (GC)], and the relative time of peak applied torque (T1 + 10, 12.5, and 15% GC) (fig. S4). Achilles tendon force was measured with a portable shear wave tensiometer placed on the left ankle for 30 s during walking with each of the 9 assistance conditions and 1 condition with the exosuit powered off (10 in total). All profiles showed a significant reduction in Achilles tendon force relative to slack, but some more than others (Fig. 5).

Of the nine conditions, condition #5 (T1 = 40% GC and T2 = 52.5% GC) showed the greatest reduction in peak Achilles tendon force. This condition was further tested to assess metabolic benefit relative to no assistance (Fig. 5). The metabolic rate during a 5-min overground route was measured for the single assistance profile and for an analogous slack bout. Similar to the prior exosuit sweep, a researcher set the pace at about 1.25 m/s to allow for comparison between trials. The chosen profile showed a 9.6% reduction in the metabolic cost of walking and a reduction in the cost of transport by 4.14% relative to the slack bout.

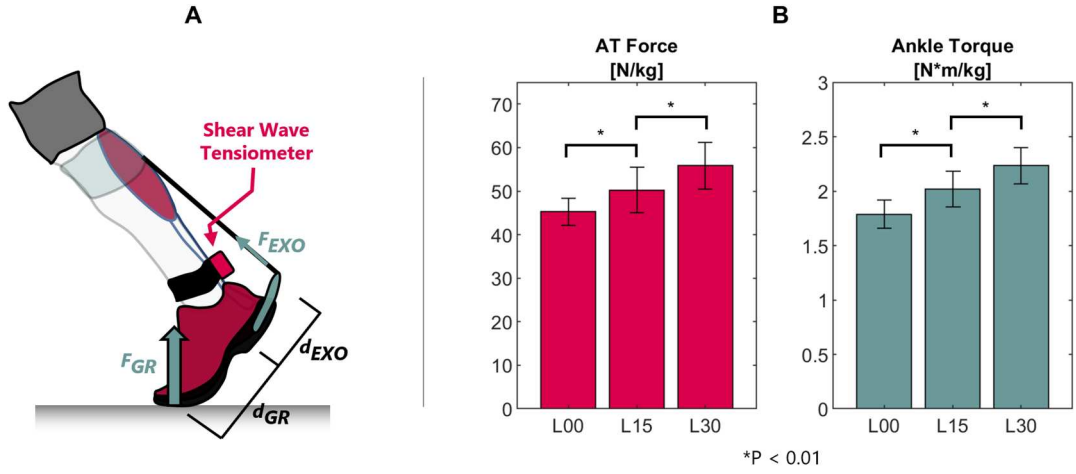

Fig. 2. Achilles tendon force and ankle torque with load carriage. (**A**) Shear wave speed in the Achilles tendon was measured with a shear wave tensiometer. Biological ankle torque was computed via inverse dynamics analysis, with the ground reaction force (F_{GR}), exosuit assistance force (F_{EXO}), and moment arms (d_{GR}, d_{EXO}) as inputs. Wave speed was used to estimate Achilles tendon force on the basis of participant-specific calibrations. (**B**) Group averages of peak Achilles tendon force and peak ankle torque exhibited significant increases with load carriage. Error bars indicate SD.

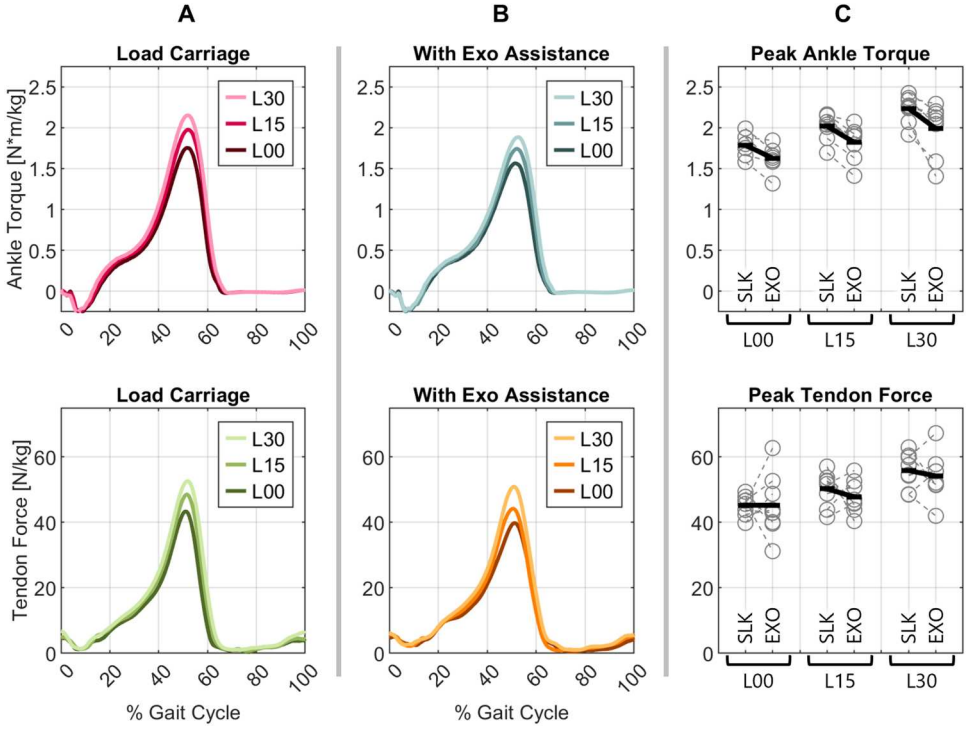

Fig. 3. Achilles tendon force and ankle torque with exosuit assistance. (**A**) Stride-averaged ankle torque and tendon force showed increases in peak magnitudes with load carriage. (**B**) Peak biological ankle torque predictably decreased with added exosuit assistance. Peak tendon force also decreased with added exosuit assistance. (**C**) Peak ankle torque and peak tendon force during pushoff are shown for each participant (gray circles with dashed lines) and as the group average (solid black lines).

DISCUSSION

This study demonstrates the use of shear wave tensiometry to characterize the modulation of Achilles tendon forces with load carriage and exosuit assistance. As hypothesized, peak Achilles tendon forces significantly increased with load carriage and were reduced with exosuit assistance (Figs. 2 and 3). However, when exosuit assistance was provided, the average reduction in tissue loading measured by tensiometry was less compared with the standard inverse dynamics estimates of biological ankle torque (Fig. 4).

Variability in biomechanical and metabolic responses to exosuit assistance is commonly encountered, inspiring substantial research into optimizing individualized assistance strategies (*6*, *30*, *31*). Our study suggests that this variability extends to internal tissue loading. Some participants (five of eight) had substantially reduced Achilles

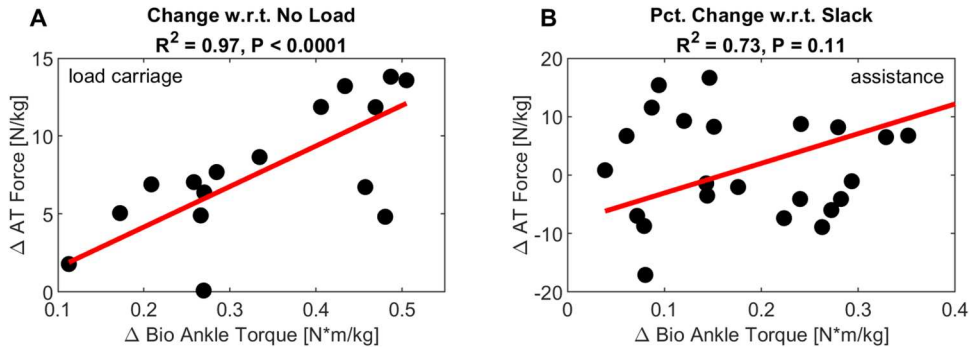

Fig. 4. Relationship between Achilles tendon force and biological ankle torque. (**A**) Achilles tendon force was correlated with biological ankle torque for load carriage conditions without exosuit assistance. (**B**) Achilles tendon force was not significantly correlated with biological ankle torque when exosuit assistance was applied. One point was excluded as an outlier (ΔBio ankle torque greater than Q3 + 1.5 × interquartile range).

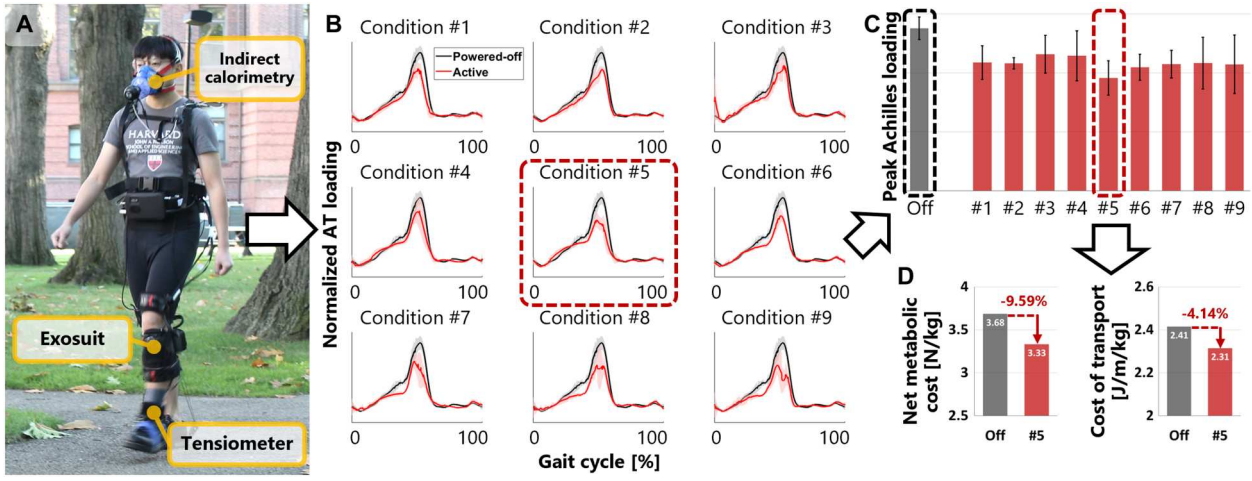

Fig. 5. Outdoor pilot results. A proof-of-concept testing of the exosuit-tensiometer combined system for overground walking in the outdoor environment. (**A**) Experimental setup. One healthy participant walked overground wearing the exosuit and the tensiometer over three walking bouts. While walking, the participant followed an investigator who kept a pace of about 1.25 m/s. (**B**) In the first bout, the exosuit changed the assistance timing parameters over 10 different conditions (powered off and 9 active conditions #1 to #9) while the tensiometer measured the Achilles tendon force. (**C**) Condition #5 (T1 = 40% GC and T2 = 52.5% GC) reduced the peak Achilles tendon force the most compared with the powered-off condition. Error bars indicate SD. (**D**) Condition #5 reduced the net metabolic cost of walking by 9.59% and the cost of transport by 4.14% compared with the powered-off condition over 5 min of walking.

tendon force during walking for at least one load carriage condition (table S1). However, other participants (three of eight) failed to have reduced Achilles tendon force (despite applied exosuit assistance) and saw little to no reduction in peak forces. This difference in response may be related to individual adaptation to the exosuit assistance parameters or, as our outdoor proof of concept would suggest, a need to tune exosuit assistance profiles. In the outdoor experiment, we considered nine assistance profiles and were able to identify an exosuit loading profile that maximized reduction in Achilles tendon force (Fig. 5). Tensiometry measurements can conceivably be done in real time and therefore may be leveraged for improving exosuit design and control for more effectively offloading Achilles tendon stress for individual participants.

Biological joint torque is traditionally used to ascertain the effects of assistance on tissue loading. Biological torque is the difference between the net joint torque determined via inverse dynamics and the torque supplied via external assistance. Our data support the idea that there can be a decoupling of peak Achilles tendon force and peak ankle torque during exosuit assistance (Fig. 4). This could be due to one or more biomechanical phenomena, such as cocontraction of antagonistic muscles (*5*, *15*, *32*), exosuit-induced changes in agonist muscle coordination (*32*), or alterations in the underlying muscle-tendon dynamics (*13*, *14*). Although the summary EMG results across participants were inconclusive, there is substantial evidence in the literature suggesting that, in general, individuals do alter their coordination patterns in the presence of exosuit assistance. For example, individuals will often activate the antagonist TA when exosuit assistance is applied at the ankle (*5*). Given that ankle torque and Achilles tendon force modulation with assistance differed, it seems that tensiometry may provide unique insights into the internal biomechanical adaptations that arise in individuals. The benefits of tuning exosuit performance to optimize the interaction between a wearer and an exosuit are widely recognized (*6*, *33*, *34*). It is conceivable that monitoring

adaptation with a tensiometer could help improve exosuit performance as well as our understanding of the relationship between peak Achilles tendon force and biological ankle torque.

Tensiometry has been validated as a tool for measuring internal forces in the tendon during walking on treadmills and overground (*17*, *18*, *21*) but has not been used to measure tendon force when exosuit assistance is being applied. Hence, we endeavored to establish confidence in the tensiometer measurements during exosuit-assisted walking. When the exosuit was turned on or off, there were immediate observable changes in the Achilles tendon wave patterns that generally adapted to a new cyclic pattern within a few strides. Although absolute wave speeds exhibited variability across participants, we did observe significant increases in wave speed with load carriage as would be expected biomechanically (Figs. 2 and 3). We performed participant-specific calibrations of wave speed to Achilles tendon force based on inverse dynamics analysis of the slack walking conditions (fig. S1). Doing calibration in this way ensured that the measurements were not affected by the donning of the exosuit. The strength of the fit between wave speed and estimated Achilles tendon force from inverse dynamics (R^2 = 0.76 to 0.99) was comparable to that we have seen in prior studies in which calibration has been done with a dynamometer or joint torques from gait analysis (*18*, *35*). One challenge is that the exosuit caused the backs of some participants' shoes to flex upward toward the tensiometer in early swing, inducing transient motion artifacts in the accelerometer signals. However, such disruptions did not affect the peak values during stance, which were the primary metrics used in this study. A remaining question is whether the dynamic transfer of exosuit forces through the musculoskeletal system affects the link between biological ankle torque and Achilles tendon force, particularly with respect to the relative timing of peak values. Further investigation is needed to elucidate this relationship and how it depends on task dynamics.

There are some limitations to consider in interpreting this work. First is that we did not consider individual variations in Achilles tendon anatomy in our tensiometry measures. Although adjusted based on ankle posture, the Achilles moment arms were estimated from generic characterizations (*18*), similar to (*20*, *23*). Furthermore, three subtendons from the SOL, MG, and LG muscles twist and merge distally into the free Achilles tendon. The exosuit footwear was designed to expose as much free Achilles tendon as possible, but access was limited in some of the shorter participants. Hence, it is feasible that in some participants, the tensiometer was positioned over or superior to the distal SOL muscle-tendon junction. There is some evidence from a cadaver study that tensiometer placement over the SOL muscle-tendon junction can affect the wave speed–force relationship (*35*), although we believe that such effects can be corrected via calibration as performed in this study.

In summary, this study shows modulation in in vivo Achilles tendon forces during walking with an ankle exoskeleton or exosuit. The modulation in Achilles tendon force with unassisted load carriage mimicked the changes in ankle torque, but Achilles tendon force modulation with exosuit assistance was more distinct from changes in biological ankle torque, indicating the need for further studies to understand muscle-tendon adaptations to external exosuit or exoskeleton assistance. The pilot outdoor study demonstrates that Achilles tendon force as measured with a wearable version of the tensiometer varies on the basis of the profile and timing of applied assistance. Shear wave tensiometry may prove useful for capturing adaptation at the musculoskeletal tissue level, which, in turn, may be useful for optimizing exosuit design and control to benefit individual participants.

MATERIALS AND METHODS

Objectives and design

The purpose of this experiment was to investigate how a powered ankle exosuit affects the loading on the Achilles tendon during walking. The study was designed to measure Achilles tendon forces during a range of load carriage and exosuit assistance conditions. Ten healthy young adult participants (five females) were recruited with institutional review board (IRB) approval (Harvard IRB #22086). One participant was excluded because of technical problems with the instrumentation, and one participant was excluded on the basis of poor ground reaction forces due to split-belt treadmill crossover.

Experimental protocol

Each individual participated in two experimental sessions: a training session and a testing session. The training session was designed to familiarize the participant with the exosuit and the load carriages used during the testing session. Motion capture, ground reactions, EMG, and tensiometry were collected during the training session to test feasibility and develop experimenter efficiency. The testing session consisted of six distinct conditions that randomly varied exosuit assistance and load carriage. The load carriages were 0, 15, and 30% body weight. The weight was carried in a backpack with shoulder and waist straps and secured to an overhead harness for safety. The backpack was worn empty for the 0% body weight load carriage conditions for consistency. The exosuit assistance magnitudes were 0 and 45% body weight, denoted as "slack" and "active" conditions. One participant included in the results was sufficiently heavy that 45% body weight exceeded the maximum force capacity of the exosuit. In this case, the assistance magnitude was reduced to 30% body weight. Each of the six conditions involved 6 min of walking. Thirty seconds of walking with the exosuit slack was collected before each assisted condition for calibration purposes. Each condition was 5 min long, and data were collected for the last 30 s of each minute. An additional 30 s at the end of each condition was used to deactivate the exosuit and stop the treadmill.

Measured outcomes

Motion capture data were captured using a lower body marker set (Qualisys, Gothenburg, Sweden; 120 Hz). Ground reaction forces were acquired using a Bertec split-belt force treadmill (Bertec, Columbus, OH, USA; 1200 Hz). Inverse dynamics was performed using Visual 3D (Visual 3D; C-Motion, Germantown, MD, USA) and custom MATLAB scripts (MathWorks, Natick, MA). EMG was measured using the Delsys Duo Sensor (Delsys, Natick, MA, USA; 1200 Hz). Electrodes were placed on the SOL, MG, LG, TA, rectus femoris, vastus medialis, vastus lateralis, and biceps femoris. The raw EMG was band-pass–filtered at 20 to 450 Hz, rectified, and low-pass–filtered at 10 Hz to calculate the EMG linear envelope. The amplitude of the EMG envelope for each muscle was normalized to the peak amplitude for that muscle measured across conditions for each participant (fig. S3). Metabolic data were collected with the Cosmed K5 portable metabolic system (Cosmed, Rome,

Italy). A shear wave tensiometer was placed on the left Achilles tendon to measure Achilles tendon force. The motion capture data acquisition, the exosuit, and the tensiometer were time-synced for each condition.

Soft exosuit

The mobile soft exosuit assisted ankle plantarflexion during walking. The system consisted of ankle-only exosuit textile architecture, mobile distal-mounted bilateral ankle actuators, and closed-loop control for walking in both indoor and outdoor environments (Fig. 1).

Apparel components

We used an updated version of the soft exosuit, similar to that in the mobile system of (*3*), in which the calf wrap components were designed to securely attach to the calves only and redistribute the pressure such that the compression over the active muscles is minimized. The exosuit textile components per leg consisted of an underlying Fabrifoam liner, a calf wrap, and an arch-shaped rigid plastic shield inserted in between to prevent compression-induced fatigue of the TA muscle. The calf wraps were similar to those previously reported by our group but redistributed the compression toward the most superior region of the shank to permit the calf muscles to bulge in a more physiologically relevant manner while walking (*36*).

Hardware implementation

On each calf, a mobile actuator was placed at the back of the calf wrap, and spooled rope was attached between the heel and calf to generate forces (*3*). On each foot, a metal bracket was bolted to the outsole of a commercial low-cut boot (Lugz Footwear, New York, NY, USA), and a custom pulley provided the distal attachment point for the rope, which looped back to a load cell on the calf wrap. Electronics and batteries to control the actuators were attached at the front of the waist. Including sensors, wires, and all accessories, all exosuit hardware components weighed 2578 g; thus, combined with the textile components described above, the total mass of the exosuit was 2960 g.

Electronics and control

The embedded electronics consisted of a two-layer control architecture with the inner layer running a position control loop and the outer layer running a force control loop, similar to (*9*). In the outer loop, assistive forces were generated in two phases: the pretension phase and the active force phase. During the pretension phase, the assistive force was passively generated by the natural ankle dorsiflexion during the mid-stance, while the motor held the rope in a fixed position. During the later active force phase, the motor actively spooled the rope position to regulate the desired force to assist with ankle pushoff. We implemented a proportional-integral force feedback controller for the active force phase (*3*).

Shear wave tensiometer

A shear wave tensiometer was used to track the changes in force in the Achilles tendon. The tensiometer consisted of a custom piezoelectric tapper (Thorlabs, Newton, NJ) that excited a traveling shear wave in the tendon. The motion of the shear wave was detected with two downstream single-axis miniature accelerometers (PCB Piezotronics, Depew, NY) separated by 8 mm. The tapper and accelerometers were housed in a custom-integrated ankle wrap. Data were recorded and processed using a custom suite of MATLAB scripts.

Shear wave speed was computed from the measured transverse tendon accelerations by performing a cross-correlation of the waveforms and dividing the resultant time delay by the physical spacing between the accelerometers. Wave speed was segmented into strides using heel strikes from inverse kinematics. Because shear wave speed is not a widely used measure of tendon loading, shear wave tensiometry studies will often use a calibration between wave speed and ankle torque to represent the tensiometry results in a more relatable way. As has been observed before (*17*, *18*, *20*, *23*), the correlation between wave speed and ankle torque for conditions without exosuit assistance allowed us to perform a calibration that related the abstract measures of wave speed to the more relatable measure of force normalized by body weight, accounting for posture-dependent changes in Achilles tendon moment arm.

For each slack trial, the Achilles tendon force was estimated by scaling ankle torques from inverse dynamics by a generic, posture-dependent Achilles moment arm (*18*). Wave speed was calibrated to estimated tendon force using the primary loading and unloading phases of the slack trials collected before each condition. This segment of the GC was defined to start at maximum plantarflexion during early stance and end at maximum plantarflexion during pushoff (fig. S1). A pragmatic approach to calibration was implemented, where either a linear or a squared relationship between wave speed and the estimated tendon force was applied, depending on which produced the strongest correlation between shear wave speed and tendon force estimated from motion analysis. Wave speed was found to predict Achilles tendon force with root mean square errors that ranged from 1.3 to 8.1 N/kg in the calibration trials. Because the Achilles tendon is unable to carry appreciable compressive loads, predictions of negative tendon force resulting from the calibration were set to zero in accordance with a slack tendon.

Statistical analysis

Statistical analyses were performed using a combination of JMP (SAS Institute, Cary, NC) and MATLAB. Significance was achieved at the $P < 0.05$ level, and Tukey post hoc tests were applied to multiple comparisons. Statistics on wave speed and tendon force were performed using the peak value during stance of each stride ($n = 24$ strides per condition), identified as subsamples, for each participant and condition. In all other cases, the mean value over all strides of a given participant and condition was used. Two-tailed t tests and linear mixed models were used to assess changes in ankle torque and Achilles tendon force with load carriage and exosuit assistance. When appropriate, participant was identified as a random variable. Muscle activation changes were assessed with analyses of variance (ANOVAs) and bivariate fits.

Supplementary Materials

This PDF file includes:
Fig. S1 to S4
Table S1

Other Supplementary Material for this manuscript includes the following:
MDAR Reproducibility Checklist

REFERENCES AND NOTES

1. B. T. Quinlivan, S. Lee, P. M. Lee, D. M. R. Lee, M. G. Lee, C. S. Lee, N. K. Lee, D. Wagner, A. Asbeck, I. G. Asbeck, C. J. Walsh, Assistance magnitude versus metabolic cost reductions for a tethered multiarticular soft exosuit. *Sci. Robot.* **2**, eaah4416 (2017).
2. P. Malcolm, S. Lee, S. Crea, C. Siviy, F. Saucedo, I. Galiana, F. A. Panizzolo, K. G. Holt, C. J. Walsh, Varying negative work assistance at the ankle with a soft exosuit during loaded walking. *J. Neuroeng. Rehabil.* **14**, 62 (2017).
3. R. W. Nuckols, S. Lee, K. Swaminathan, D. Orzel, R. D. Howe, C. J. Walsh, Individualization of exosuit assistance based on measured muscle dynamics during versatile walking. *Sci. Robot.* **6**, eabj1362 (2021).
4. S. H. Collins, M. Bruce Wiggin, G. S. Sawicki, Reducing the energy cost of human walking using an unpowered exoskeleton. *Nature* **522**, 212–215 (2015).
5. R. W. Nuckols, G. S. Sawicki, Impact of elastic ankle exoskeleton stiffness on neuromechanics and energetics of human walking across multiple speeds. *J. Neuroeng. Rehabil.* **17**, 75 (2020).
6. J. Zhang, P. Fiers, K. A. Witte, R. W. Jackson, K. L. Poggensee, C. G. Atkeson, S. H. Collins, Human-in-the-loop optimization of exoskeleton assistance during walking. *Science* **356**, 1280–1284 (2017).
7. L. N. Awad, J. Bae, K. O'Donnell, S. M. M. de Rossi, K. Hendron, L. H. Sloot, P. Kudzia, S. Allen, K. G. Holt, T. D. Ellis, C. J. Walsh, A soft robotic exosuit improves walking in patients after stroke. *Sci. Transl. Med.* **9**, eaai9084 (2017).
8. L. N. Awad, J. Bae, P. Kudzia, A. Long, K. Hendron, K. G. Holt, K. O?Donnell, T. D. Ellis, C. J. Walsh, Reducing circumduction and hip hiking during hemiparetic walking through targeted assistance of the paretic limb using a soft robotic exosuit. *Am. J. Phys. Med. Rehabil.* **96**, S157–S164 (2017).
9. C. Siviy, J. Bae, L. Baker, F. Porciuncula, T. Baker, T. D. Ellis, L. N. Awad, C. J. Walsh, Offline assistance optimization of a soft exosuit for augmenting ankle power of stroke survivors during walking. *IEEE Robot. Autom. Lett.* **5**, 828–835 (2020).
10. K. Z. Takahashi, M. D. Lewek, G. S. Sawicki, A neuromechanics-based powered ankle exoskeleton to assist walking post-stroke: A feasibility study. *J. Neuroeng. Rehabil.* **12**, 23 (2015).
11. S. S. Fricke, C. Bayón, H. van der Kooij, E. H. Edwin, Automatic versus manual tuning of robot-assisted gait training in people with neurological disorders. *J. Neuroeng. Rehabil.* **17**, 9 (2020).
12. N. L. Tagliamonte, A. R. Wu, I. Pisotta, F. Tamburella, M. Masciullo, M. Arquilla, E. H. F. van Asseldonk, H. van der Kooij, F. Dzeladini, A. J. Ijspeert, M. Molinari, Benefits and potential of a neuromuscular controller for exoskeleton-assisted walking, in *Biosystems and Biorobotics* (Springer Science and Business Media Deutschland GmbH, 2022), vol. 27, pp. 281–285.
13. R. W. Nuckols, T. J. M. Dick, O. N. Beck, G. S. Sawicki, Ultrasound imaging links soleus muscle neuromechanics and energetics during human walking with elastic ankle exoskeletons. *Sci. Rep.* **10**, 3604 (2020).
14. R. W. Jackson, C. L. Dembia, S. L. Delp, S. H. Collins, Muscle-tendon mechanics explain unexpected effects of exoskeleton assistance on metabolic rate during walking. *J. Exp. Biol.* **220**, 2082–2095 (2017).
15. G. S. Sawicki, N. S. Khan, A simple model to estimate plantarflexor muscle–tendon mechanics and energetics during walking with elastic ankle exoskeletons. *IEEE Trans. Biomed. Eng.* **63**, 914–923 (2016).
16. M. B. Yandell, B. T. Quinlivan, D. Popov, C. Walsh, K. E. Zelik, Physical interface dynamics alter how robotic exosuits augment human movement: Implications for optimizing wearable assistive devices. *J. Neuroeng. Rehabil.* **14**, 40 (2017).
17. J. A. Martin, S. C. E. Brandon, E. M. Keuler, J. R. Hermus, A. C. Ehlers, D. J. Segalman, M. S. Allen, D. G. Thelen, Gauging force by tapping tendons. *Nat. Commun.* **9**, 1592 (2018).
18. E. M. Keuler, I. F. Loegering, J. A. Martin, J. D. Roth, D. G. Thelen, Shear wave predictions of Achilles tendon loading during human walking. *Sci. Rep.* **9**, 13419 (2019).
19. A. Ebrahimi, I. F. Loegering, J. A. Martin, R. L. Pomeroy, J. D. Roth, D. G. Thelen, Achilles tendon loading is lower in older adults than young adults across a broad range of walking speeds. *Exp. Gerontol.* **137**, 110966 (2020).
20. A. Ebrahimi, R. L. Kuchler, R. L. Pomeroy, I. F. Loegering, J. A. Martin, D. G. Thelen, Normative Achilles and patellar tendon shear wave speeds and loading patterns during walking in typically developing children. *Gait Posture* **88**, 185–191 (2021).
21. S. E. Harper, R. A. Roembke, J. D. Zunker, D. G. Thelen, P. G. Adamczyk, Wearable tendon kinetics. *Sensors* **20**, 4805 (2020).
22. S. E. Harper, D. G. Schmitz, P. G. Adamczyk, D. G. Thelen, Fusion of wearable kinetic and kinematic sensors to estimate triceps surae work during outdoor locomotion on slopes. *Sensors.* **22**, 1589 (2022).
23. A. Ebrahimi, M. H. Schwartz, J. A. Martin, T. F. Novacheck, D. G. Thelen, Atypical triceps surae force and work patterns underlying gait in children with cerebral palsy. *J. Orthop. Res.* , (2022).
24. S. A. Birrell, R. H. Hooper, R. A. Haslam, The effect of military load carriage on ground reaction forces. *Gait Posture* **26**, 611–614 (2007).
25. G. K. Lenton, T. L. A. Doyle, D. G. Lloyd, J. Higgs, D. Billing, D. J. Saxby, Lower-limb joint work and power are modulated during load carriage based on load configuration and walking speed. *J. Biomech.* **83**, 174–180 (2019).
26. T. S. Buchanan, D. G. Lloyd, K. Manal, T. F. Besier, Neuromusculoskeletal modeling: Estimation of muscle forces and joint moments and movements from measurements of neural command. *J. Appl. Biomech.* **20**, 367–395 (2004).
27. E. Harman, K. H. Han, P. Frykman, C. Pandorf, The effects of backpack weight on the biomechanics of load carriage. *Security*, 71 (2000).
28. M. K. MacLean, D. P. Ferris, Human muscle activity and lower limb biomechanics of overground walking at varying levels of simulated reduced gravity and gait speeds. *PLOS ONE* **16**, e0253467 (2021).
29. N. Murray, D. Cipriani, D. O'Rand, R. Reed-Jones, Effects of foot position during squatting on the quadriceps femoris: An electromyographic study. *Int. J. Exerc. Sci.* **6**, 114–125 (2013).
30. S. Song, S. H. Collins, Optimizing exoskeleton assistance for faster self-selected walking. *IEEE Trans. Neural Syst. Rehabil. Eng.* **29**, 786–795 (2021).
31. H. Han, W. Wang, F. Zhang, X. Li, J. Chen, J. Han, J. Zhang, Selection of muscle-activity-based cost function in human-in-the-loop optimization of multi-gait ankle exoskeleton assistance. *IEEE Trans. Neural Syst. Rehabil. Eng.* **29**, 944–952 (2021).
32. K. M. Steele, R. W. Jackson, B. R. Shuman, S. H. Collins, Muscle recruitment and coordination with an ankle exoskeleton. *J. Biomech.* **59**, 50–58 (2017).
33. K. A. Ingraham, C. D. Remy, E. J. Rouse, User preference of applied torque characteristics for bilateral powered ankle exoskeletons, in *Proceedings of the IEEE RAS and EMBS International Conference on Biomedical Robotics and Biomechatronics* (IEEE Computer Society, 2020), vol. 2020-Novem, pp. 839–845.
34. J. R. Koller, C. D. Remy, D. P. Ferris, Biomechanics and energetics of walking in powered ankle exoskeletons using myoelectric control versus mechanically intrinsic control. *J. Neuroeng. Rehabil.* **15**, 42 (2018).
35. J. A. Martin, M. W. Kindig, C. J. Stender, W. R. Ledoux, D. G. Thelen, Calibration of the shear wave speed-stress relationship in in situ Achilles tendons using cadaveric simulations of gait and isometric contraction. *J. Biomech.* **106**, 109799 (2020).
36. E. Azizi, E. L. Brainerd, T. J. Roberts, Variable gearing in pennate muscles. *Proc. Natl. Acad. Sci. U.S.A.* **105**, 1745–1750 (2008).

Acknowledgments: We would like to thank J. Foster, A. Eckert Erdheim, D. Orzel, S. Cone, and K. Peregrine for technical assistance during preparation and execution of the study. **Funding:** This material is based on work sponsored by the NSF Disability and Rehabilitation Engineering (DARE) grant 2019621 and the NSF Graduate Research Fellowship Program (GRFP) fellowships DGE-1747503 and DGE-1650114. **Author contributions:** Conceptualization: D.G.S., R.W.N., S.L., T.A., K.S., C.J.W., and D.G.T. Methodology: D.G.S., R.W.N., S.L., T.A., C.J.W., and D.G.T. Investigation: D.G.S., R.W.N., S.L., T.A., K.S., C.J.W., and D.G.T. Formal analysis: D.G.S., R.W.N., and S.L. Visualization: D.G.S., R.W.N., and S.L. Resources: D.G.S., R.W.N., S.L., and T.A. Software: D.G.S., R.W.N., and S.L. Funding acquisition: D.G.S., R.W.N., S.L., C.J.W., and D.G.T. Project administration: D.G.S., R.W.N., S.J.W., T.A., C.J.W., and D.G.T. Supervision: C.J.W. and D.G.T. Writing—original draft: D.G.S. and R.W.N. Writing—review and editing: D.G.S., R.W.N., S.L., T.A., K.S., C.J.W., and D.G.T. **Competing interests:** S.L. and C.J.W. are patent authors for the design of the ankle exoskeletons used in this experiment (US10434030B2). D.G.T. is a patent author for the design of the shear wave tensiometry used in this experiment (US10631775B2). All other authors declare that they have no competing interests. **Data and materials availability:** All data needed to support the conclusions of this manuscript are included in the main text or the Supplementary Materials. Data and code can be accessed in the permanent repository (10.5281/zenodo.7106097).

Submitted 25 March 2022
Accepted 26 September 2022
Published 19 October 2022
10.1126/scirobotics.abq1514

Science Robotics

Modulation of Achilles tendon force with load carriage and exosuit assistance

Dylan G. SchmitzRichard W. NuckolsSangjun LeeTunc AkbasKrithika SwaminathanConor J. WalshDarryl G. Thelen

Sci. Robot., 7 (71), eabq1514. • DOI: 10.1126/scirobotics.abq1514